2012

Selecting sprinkler packages for center pivots

Derrel L. Martin
University of Nebraska- Lincoln, derrel.martin@unl.edu

William L. Kranz
University of Nebraska-Lincoln, wkranz1@unl.edu

Allen L. Thompson
University of Missouri, Columbia, ThompsonA@missouri.edu

Hong Liang
Northeast Forestry University, Harbin, China

SELECTING SPRINKLER PACKAGES FOR CENTER PIVOTS

D. L. Martin, W. L. Kranz, A. L. Thompson, H. Liang

ABSTRACT. *Center pivots are the primary method of irrigation across the U.S. Great Plains. Center-pivot irrigation is also the fastest growing method of irrigation in the U.S. and around the world. Pivots have the potential to be very efficient and uniform if sprinkler devices are properly selected for local field conditions. New water application devices provide for selection that minimizes runoff and controls droplet sizes to reduce evaporation and drift losses. We present updates to models for computing runoff potential based on characteristics of sprinkler devices and soil textural classes. A dimensionless solution to the Green-Ampt infiltration method for center pivots is presented to better understand factors that influence runoff. That analysis shows that two dimensionless factors are needed to assess the runoff potential. One scaling factor is based on system design, and the second factor is based on irrigation management. An evaporation routine has also been incorporated to estimate potential evaporation losses that may result from utilization of a specific sprinkler design. Modeling runoff and evaporative losses simultaneously allows for comparison of tradeoffs in sprinkler package selection.*

Keywords. *Center-pivot irrigation, Evaporative loss, Runoff, Sprinkler selection.*

The expansion of center pivots during the past several decades has far exceeded the growth of other methods of irrigation. Currently, center pivots are used on more than ten million hectares in the U.S. and account for approximately 47% of the land irrigated, according to the latest USDA survey (FRIS, 2008). Pivots have been popular because of their ease of management and potential for high application efficiency. Energy costs for pumping and pressurizing irrigation water have increased dramatically during the last decade, which has heightened interest in attaining high application efficiencies. Simultaneously, the irrigation industry has developed new water application devices for center pivots. These developments provide designers and irrigators with many choices for the sprinkler package used on the pivot.

Proper selection and operation of the sprinkler package is critical to achieving the potential application efficiency of center pivots. Four factors are important in selecting sprinkler packages: (1) operating pressure, (2) uniformity of application, (3) runoff potential, and (4) evaporation losses during water application. The lowest operating pressure that achieves high uniformity and efficiency is the most desirable, and thus depends on the performance of the last three factors. Crop characteristics and producer management practices also affect the actual efficiency.

Heermann et al. (1999) studied the effect of application pattern shape on center-pivot irrigation uniformity. They analyzed four distribution patterns (triangular, elliptical, donut-shaped, and piecewise linear) typical of devices that apply peak application depths away from the nozzle. They found that the spacing of sprinkler devices was more important than the pattern shape for individual sprinklers in achieving uniform water application. Elliptical patterns, typical of impact sprinklers with spreader nozzles, consistently resulted in the highest uniformity, while donut-shaped patterns resulted in the lowest. Device spacing for donut-shaped patterns had to be reduced compared to other devices to attain an acceptable coefficient of uniformity. Simulation of the effect of sprinkler spacing of currently available water application devices has been included in the CPED model by Heermann and Stahl (2006).

We developed a simulation model (CPNozzle) to simulate the potential runoff from sprinkler packages on center pivots. The early version was based on the NRCS intake family similar to that developed by Gilley (1984). We expanded the model to include an infiltration model based on the Green-Ampt method, building on the procedures of Hachum and Alfaro (1980). Both of these developments were based on earlier sprinkler models. Bai (2001) used a simulation program to compare the potential runoff for

Submitted for review in September 2011 as manuscript number SW 9400; approved for publication by the Soil & Water Division of ASABE in November 2011. Presented at the 5th National Decennial Irrigation Conference as Paper No. IRR109282.

Mention of trade name, proprietary product, or specific equipment does not constitute a guarantee or warranty by the authors or their institutions and does not imply approval of product to the exclusion of others that may be suitable.

The authors are **Derrel L. Martin, ASABE Fellow,** Professor, Department of Biological System Engineering, University of Nebraska-Lincoln, Lincoln, Nebraska; **William L. Kranz, ASABE Member,** Associate Professor, Northeast Research and Extension Center, University of Nebraska, Concord, Nebraska; **Allen L. Thompson, ASABE Member,** Associate Professor, Department of Biological Engineering, University of Missouri, Columbia, Missouri; and **Hong Liang,** Visiting Professor, School of Forestry, Northeast Forestry University, Harbin, China. **Corresponding author:** Derrel L. Martin, Department of Biological System Engineering, University of Nebraska-Lincoln, 243 L.W. Chase Hall, Lincoln, NE 68583-0726; phone: 402-472-1586; e-mail: dlmartin @unlnotes.unl.edu.

  ISSN 2151-0032

sprinklers with a range of individual distribution patterns. He showed that the simulated runoff from overlapping individual sprinklers produced nearly the same amount of potential runoff as when an elliptical shape was used for the pattern of the package as a whole. We have combined the Green-Ampt infiltration procedure with an elliptical application pattern for the combined sprinkler package to develop scaled predictions of runoff based on dimensionless parameters. These solutions can be used to provide guidelines for sprinkler package selection and management of the application depth of the pivot.

Thompson et al. (1997) used a simulation model to predict the fraction of the water application that evaporates in the air before reaching the crop surface, the amount of water that is intercepted and evaporated from the crop canopy, and the amount of water that evaporates from the soil surface. Earlier results showed that evaporation losses are strongly influenced by the size of the water droplets, the temperature of the irrigation water, and ambient micrometeorological conditions. Transpiration decreased considerably when intercepted water on the canopy was available to evaporate. The amount of water evaporated from the canopy offsets the water use for transpiration, and therefore canopy evaporation should not be considered a total loss. In this article, we updated information for sprinkler models and developed estimates of evaporative losses for some typical sprinkler packages used on pivots today.

Other research on the efficiency of center-pivot irrigation has focused on predicting runoff, evaporation losses, and uniformity of water application. Some efforts have focused on measuring runoff for selected fields with a limited number of sprinkler devices and system configurations. Developments by DeBoer and Chu (2001), Luz and Heermann (2005), and Silva (2007) are examples of discrete measurements of runoff that have been generalized to some extent. Other authors have developed simulation programs for uniformity or runoff (Kincaid et al., 1969; Gilley, 1984; DeBoer et al., 1988; Valin and Pereira, 2006; Delirhasannia et al., 2010), while others have built models of the evaporation process. Few researchers have combined runoff and evaporation simulation to estimate the effect of sprinkler package design on the overall efficiency of a center-pivot irrigation system. Many models are designed to provide simulation results for one soil-system combination. While that is useful to the user, it does not provide an overview of the process, and it requires several simulations to evaluate alternatives. While we have developed a similar model, we have generalized results in this article to show how important parameters affect the water application efficiency of center pivots.

RUNOFF ANALYSIS

Irrigation water that is applied at a rate that exceeds the infiltration rate of the soil accumulates in the depressions and surface roughness in the field. When the local surface storage is filled, the excess application flows downhill, where it may accumulate in low spots or flow from the irrigated field. Center pivots apply water at high rates, especially near the distal end of the pivot. The water application rate for an elliptical application pattern for the sprinkler package is given by:

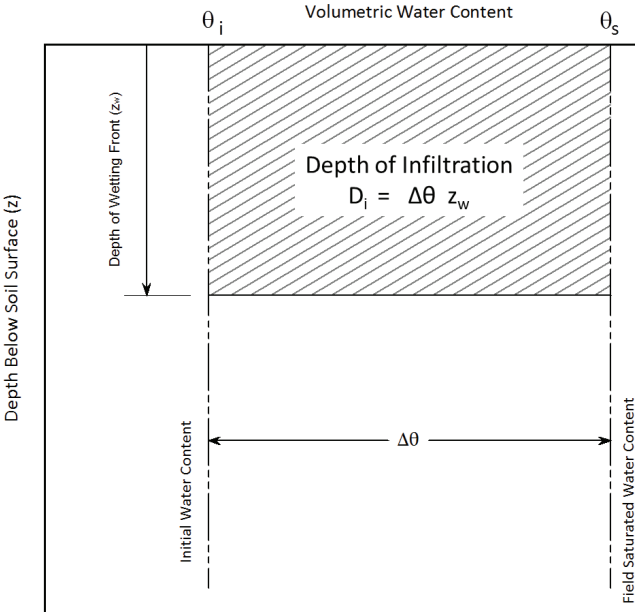

Figure 1. Diagram of Green-Ampt infiltration method.

$$R = \frac{2R_p}{T_w}\sqrt{T_w t - t^2} = 2R_p\sqrt{\tau - \tau^2},\ 0 < \tau < 1 \qquad (1)$$

where R is the rate of water application, R_p is the peak rate of application, t is the elapsed time of water application at the specified point, and T_w is the duration of water application (or time of wetting) at the point under the center pivot for the selected depth of application. The dimensionless parameter (τ) is the ratio of the elapsed time relative to the time of wetting.

The infiltration rate for the Green-Ampt method is given by:

$$I = K_s\left(1 + \frac{\Delta\theta G}{D_i}\right) \qquad (2)$$

where I is the infiltration rate, K_s is the effective hydraulic conductivity, G is the capillary drive, and D_i is the depth of water infiltrated at time t. The effective hydraulic conductivity represents the field-saturated conductivity, which is frequently referred to as the satiated conductivity. The value is often about 90% of the truly saturated conductivity. If the initial soil water content at the start of the irrigation is constant over the relevant depth, then the change in volumetric water content during infiltration is represented by the value of $\Delta\theta = \theta_s - \theta_i$, as illustrated in figure 1. This development assumes that the soil properties are uniform with depth.

The capillary drive is traditionally determined as:

$$G = \frac{1}{K_s - K_i}\int_{h_i}^{0} K(h)dh \approx \frac{1}{K_s}\int_{\infty}^{0} K(h)dh \qquad (3)$$

where $K(h)$ is the hydraulic conductivity as a function of the capillary pressure head (h), and K_s is the saturated hy-

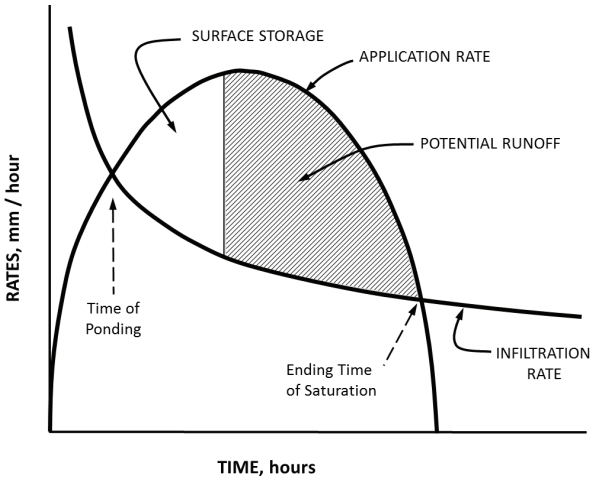

Figure 2. Interaction between rate of water application and the infiltration rate of the soil.

draulic conductivity. Subscript *i* refers to the initial head and conductivity before irrigating.

The time when the soil surface first becomes saturated and water begins to pond occurs when the water application rate equals the infiltration rate. As illustrated in figure 2, prior to the time of saturation, the infiltration potential exceeds the application rate, and no runoff occurs. After ponding begins, the excess water application becomes available for filling surface storage and eventually may result in runoff once the surface storage is filled.

The relative time of ponding (τ_p) can be determined by equating the infiltration and application rates from equations 1 and 2:

$$2R_p\sqrt{\tau_p-\tau_p^2}=K_s\left(1+\frac{\Delta\theta G}{D_p}\right) \tag{4}$$

At the time of ponding, the depth of infiltration (D_p) equals the depth of application. The depth of water applied after time (t) is determined by integrating the application rate to give:

$$\begin{aligned} D(\tau) &= D_a\left(\frac{2}{\pi}\right)\left[(2\tau-1)\sqrt{\tau-\tau^2}\right. \\ &\quad \left.+\frac{1}{2}\sin^{-1}(2\tau-1)+\frac{\pi}{4}\right] \\ &= D_a f(\tau) \end{aligned} \tag{5}$$

where D_a is the total depth of water applied.

Combining equations 4 and 5 gives the following relationship for when the application rate equals the infiltration rate:

$$2\alpha\sqrt{\tau_p-\tau_p^2}=1+\frac{\beta}{f(\tau_p)} \tag{6}$$

where $\alpha = R_p/K_s$, $\beta = (\Delta\theta G)/D_a$, and the fraction of the total depth applied by relative time τ is represented by $f(\tau)$ as in equation 5. Equation 6 can be solved numerically to determine the time of ponding for specific values of α and β. The results in figure 3 illustrate that the time of ponding occurs very early in the irrigation if the peak application rate is more than ten times the effective saturated hydraulic conductivity of the soil. The relative time of ponding reaches an asymptote for low peak application rates. The asymptotic limit depends on the volumetric water content change times the capillary drive relative to the total depth of application. Large application depths correspond to lower values of parameter β and, as expected, ponding occurs at an earlier relative time in the irrigation event for large application depths.

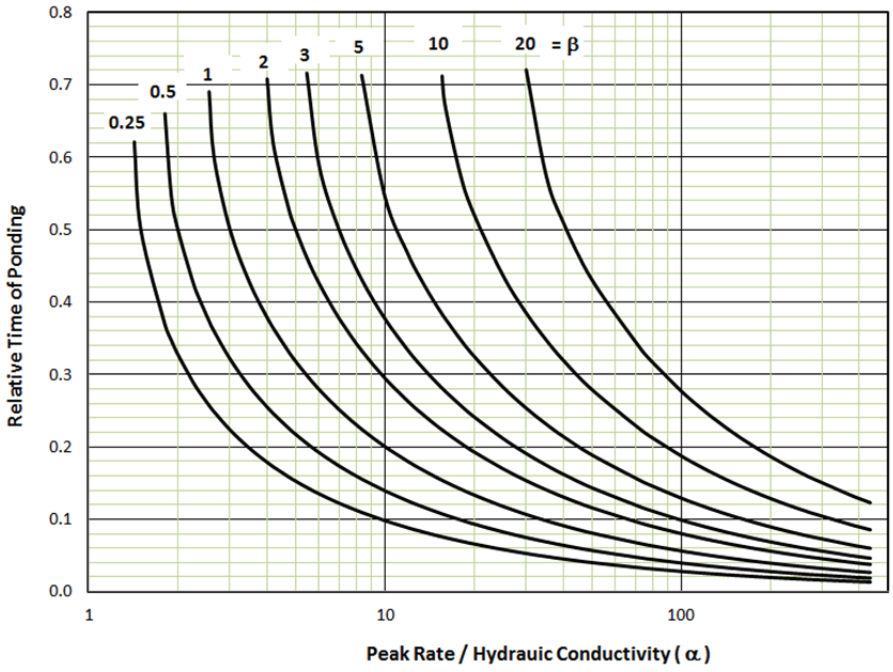

Figure 3. Solution for the relative time of ponding (τ_p).

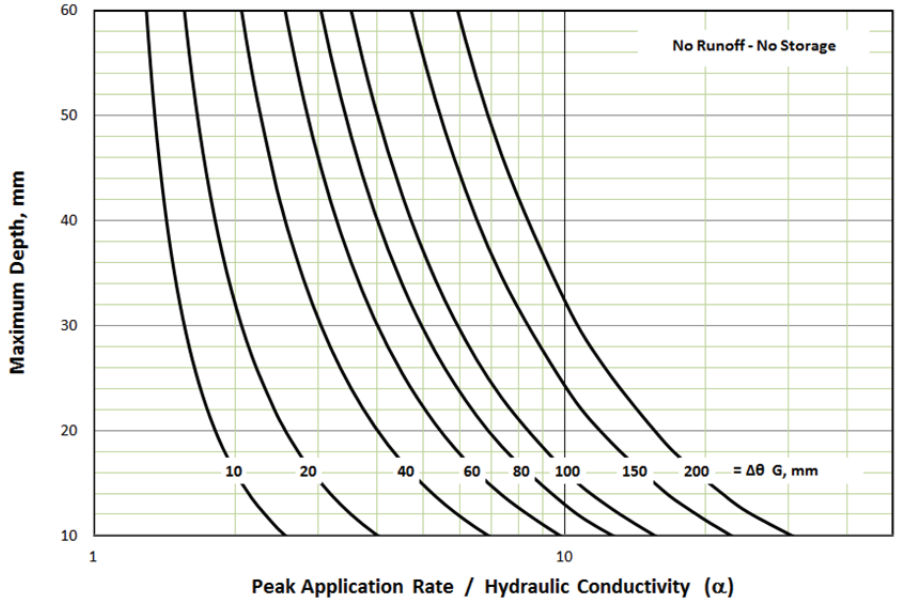

Figure 4. Maximum application depth that can be applied without runoff when there is no surface storage.

The maximum depth of application that can be applied without runoff when no surface storage is available can be determined where the infiltration rate is tangential to the application rate, or where the slope of the infiltration rate equals the slope of the application rate and is given by:

$$\frac{dR}{dt}=\left(\frac{R_p}{T_w}\right)\left(\frac{1-2\tau_o}{\sqrt{\tau_o-\tau_o^2}}\right)=\frac{dI}{dt}=-\left(\frac{2\pi\beta K}{T_w}\right)$$

$$\times\left[\frac{\sqrt{\tau_o-\tau_o^2}}{\left((2\tau_o-1)\sqrt{\tau_o-\tau_o^2}+\frac{1}{2}\sin^{-1}(2\tau_o-1)+\frac{\pi}{4}\right)^2}\right] \quad (7)$$

At this time, the surface just reaches saturation since the rate of application equals the infiltration rate. Combining equations 6 and 7 yields an expression to determine the maximum depth of application that can be applied without runoff when there is no surface storage:

$$\alpha=\left[8\left(\tau_o-\tau_o^2\right)\right]\div\left\{16\left(\tau_o-\tau_o^2\right)^{3/2}-2(2\tau_o-1)\right.$$

$$\left.\times\left[(2\tau_o-1)\sqrt{\tau_o-\tau_o^2}+\frac{1}{2}\sin^{-1}(2\tau_o-1)+\frac{\pi}{4}\right]\right\} \quad (8)$$

where τ_o is the relative time for no runoff when no surface storage is available. Iterative solution of equation 8 for a given α provides the relative time τ_o. The maximum depth of application that can be applied for no runoff when there is no surface storage is computed from solution of equation 7 for the corresponding value of β at time τ_o:

$$\beta=\frac{\alpha\pi(2\tau_o-1)f^2(\tau_o)}{8\left(\tau_o-\tau_o^2\right)} \quad (9)$$

From the definition of β, we can determine the maximum depth of application that will not produce runoff when there is no surface storage:

$$D_o=\left(\frac{8\Delta\theta G}{\pi\alpha}\right)\frac{\left(\tau_o-\tau_o^2\right)}{(2\tau_o-1)f^2(\tau_o)} \quad (10)$$

Note that the maximum application depth is only a function of the ratio of the peak application rate to the effective saturated hydraulic conductivity and the product of the volumetric water content increase and the capillary drive. This allows for expressing the maximum depth in a single graph, as in figure 4.

Determination of the potential runoff requires the time when the rate of application falls below the ability of the soil to infiltrate water and the volume of water stored on the soil begins to diminish. This is near the end of the application excess period (t_e) and is determined by equating the application rate and the infiltration rate when the relative time is greater than τ_o. The solution is different from that described in equation 4 because the depth of infiltration no longer equals the depth of water applied. The depth of infiltration can be determined by integrating:

$$I=\frac{dD_i}{dt}=K\left(1+\frac{\Delta\theta G}{D_i}\right)$$

$$\int_{t_p}^{t}\frac{dK}{dt}=\int_{D_p}^{D_i}\left[\frac{D_i}{D_i+\Delta\theta G}\right]dD_i$$

and

which gives:

$$D_i=D_p+\Delta\theta G\ln\left[\frac{D_i+\Delta\theta G}{D_p+\Delta\theta G}\right]+K\left(t-t_p\right)$$

and dividing by D_a gives:

$$\delta = f(\tau_p) + \beta \ln\left[\frac{\delta + \beta}{f(\tau_p) + \beta}\right] + \frac{4}{\pi\alpha}(\tau - \tau_p)$$

$$\text{for } \tau_p < \tau < \tau_e \tag{11}$$

where $\delta = D_i/D_a$, $\tau_e = t_e/T_w$, and the other variables are as previously defined. The application rate and the infiltration rates are equal at relative time τ_e, which gives:

$$2\alpha\sqrt{\tau_e - \tau_e^2} = 1 + \frac{\beta}{\delta_e} \tag{12}$$

where τ_e is the relative time at the end of pond development, and δ_e is the ratio of the depth of water infiltrated at the end of ponding relative to the depth of water applied for the irrigation ($\delta_e = D_{ie}/D_a$). The relative depth (δ_e) can be computed from equation 11 when combined with equation 12 to determine τ_e from the known values of α and β:

$$\left(\frac{\beta}{2\alpha\sqrt{\tau_e - \tau_e^2} - 1}\right) = f(\tau_p) + \beta \ln\left[\frac{\beta\left(\frac{1}{2\alpha\sqrt{\tau_e - \tau_e^2} - 1} + 1\right)}{f(\tau_p) + \beta}\right] + \frac{4(\tau_e - \tau_p)}{\pi\alpha} \tag{13}$$

The value of τ_e can be determined through numerical methods for known values of α and β. Note that $\tau_o \le \tau_e \le 1$.

Finally, the potential runoff (P) can be determined by integrating the difference between the application rate and the infiltration rate over the time interval (t_p, t_e):

$$P = D_a[f(\tau_e) - \delta_e]$$

and from equation 12:

$$\frac{P}{D_a} = \left[f(\tau_e) - \frac{\beta}{2\alpha\sqrt{\tau_e - \tau_e^2} - 1}\right] \tag{14}$$

The end of ponding (τ_e) and the fraction of the application that could potentially run off are only functions of α and β.

Pivot Relationships

The scaling factors (α and β) depend on the characteristics and management of the pivot. The peak application rate depends on the pivot design:

$$R_p = \frac{4C_g r}{W_r} \tag{15}$$

where C_g is the gross system capacity (i.e., the total flow into the pivot divided by the area irrigated in the field with resulting units of length per unit time), r is the distance from the pivot base to the point of interest, and W_r is the wetted radius of the elliptical sprinkler package at the point of interest. The wetted radius is determined by the operating pressure of the sprinkler device and the flow required for the sprinkler at a point along the pivot lateral.

The length of time that water is applied at the point of interest, i.e., the time of wetting, is determined by:

$$T_w = \left(\frac{W_r}{\pi r}\right)\left(\frac{D_a}{C_g}\right) \tag{16}$$

Thus, the scaling factor (α) is given by:

$$\alpha = \frac{R_p}{K_S} = \frac{4C_g r}{K_S W_r} \tag{17}$$

This illustrates that α increases with distance from the pivot and is inversely related to the wetted radius of the sprinklers installed near the point of interest. Scaling factor α is clearly a design parameter and is not affected by system management. It does depend on the effective hydraulic conductivity of the soil.

The second scaling factor (β) depends on irrigation management and soil properties, and not on pivot design:

$$\beta = \frac{\Delta\theta G}{D_a} \tag{18}$$

The capillary drive, and to some extent $\Delta\theta$, are properties of the soil. The application depth (D_a) and $\Delta\theta$ depend on management decisions. The value of β is small for sandy soils, large application depths, and when the soil is wet at the time of irrigation. Conversely, β is large for fine-textured soils, small application depths, and dry soils.

Soil Properties

Runoff calculations depend on the properties of the soil. While soil properties vary considerably, characteristics for soil textural classes are instructive in evaluating the runoff potential (table 1 and 2). The combined parameter ($\Delta\theta G$) was computed for three levels of management allowed depletion (MAD). The results in table 2 show that the combined parameter is not overly sensitive to variation in the initial soil water content at the time of irrigation. Users can probably select an average value for estimating the fraction of the water application that could run off or that will need to be stored on the soil surface. The irrigation management scaling factor (β) that corresponds to the MAD value of 50% varies from a low value of about 0.5 to almost 10 for various application depths and soils. The irrigation management scaling factor varies about one order of magnitude for the conditions presented in table 2.

Variation of the irrigation design scaling factor (α) for the mean hydraulic conductivity is also shown in table 2 for

Table 1. Approximate soil properties for eleven soil texture classes (adapted from Kozak and Ahuja, 2005, and Rawls et al., 1982).

Texture Class	Effective Hydraulic Conductivity (mm h^{-1})	Pore Size Distribution Index	Geometric Mean Bubbling Pressure (mm)	Capillary Drive (mm) From Kozak and Ahuja (2005)	Capillary Drive (mm) From Rawls et al. (1982)	Volumetric Water Content (m^3 m^{-3}) Porosity	Effective Saturation	Field Capacity	Wilting Point	Available Water Capacity (mm m^{-1})
Sand	200.0	0.591	74	101	50	0.44	0.42	0.12	0.04	80
Loamy sand	61.0	0.474	89	125	70	0.44	0.40	0.18	0.08	100
Sandy loam	25.0	0.322	149	226	130	0.45	0.41	0.22	0.10	120
Loam	13.0	0.220	114	182	110	0.46	0.43	0.26	0.11	150
Silt loam	7.0	0.210	212	342	200	0.50	0.49	0.33	0.15	180
Sandy clay loam	4.5	0.250	286	450	260	0.40	0.36	0.33	0.18	155
Clay loam	2.5	0.194	264	431	260	0.46	0.39	0.34	0.20	140
Silty clay loam	1.5	0.151	332	561	350	0.47	0.43	0.34	0.19	150
Sandy clay	1.2	0.168	297	495	300	0.43	0.39	0.34	0.22	120
Silty clay	1.0	0.127	349	601	380	0.48	0.43	0.41	0.27	140
Clay	0.6	0.131	380	653	410	0.48	0.39	0.36	0.24	120

Table 2. Irrigation design and management properties for eleven soil texture classes.

Texture Class	$\Delta\theta$ for MAD values of: 75%	50%	25%	$\Delta\theta G$ (mm) based on Kozak and Ahuja (2005) for MAD values of: 75%	50%	25%	β for MAD value of 50% and application depths (mm) of: 10	25	50	α for peak application rates (mm h^{-1}) of: 100	50	25
Sand	0.36	0.34	0.32	36	34	32	3.4	1.4	0.68	0.50	0.25	0.13
Loamy sand	0.30	0.27	0.25	37	34	31	3.4	1.4	0.68	1.6	0.82	0.41
Sandy loam	0.28	0.25	0.22	64	57	50	5.7	2.3	1.1	4.0	2.0	1.0
Loam	0.29	0.25	0.21	52	45	39	4.5	1.8	0.91	7.7	3.8	1.9
Silt loam	0.29	0.25	0.20	99	84	69	8.4	3.4	1.7	14	7.1	3.6
Sandy clay loam	0.15	0.11	0.07	66	48	31	4.8	1.9	1.0	22	11	5.6
Clay loam	0.16	0.12	0.09	67	52	37	5.2	2.1	1.0	40	20	10
Silty clay loam	0.20	0.17	0.13	115	94	73	9.4	3.7	1.9	67	33	17
Sandy clay	0.14	0.11	0.08	69	54	40	5.4	2.2	1.1	83	42	21
Silty clay	0.13	0.09	0.06	76	55	34	5.5	2.2	1.1	100	50	25
Clay	0.12	0.09	0.06	75	56	36	5.6	2.2	1.1	167	83	42

Table 3. Surface storage (mm) due to residue level and land slope (NRCS, 2005).

Residue Cover (%)	Storage Due to Residue (mm)	Field Slope (%) 0.5	1	1.5	2	2.5	3	3.5	4	5
0	0.0	12.7	11.2	9.7	7.6	6.6	5.1	4.1	2.5	0.0
10	0.3	13.0	11.4	9.9	7.9	6.9	5.3	4.3	2.8	0.3
20	0.8	13.5	11.9	10.4	8.4	7.4	5.8	4.8	3.3	0.8
30	1.8	14.5	13.0	11.4	9.4	8.4	6.9	5.8	4.3	1.8
40	3.0	15.7	14.2	12.7	10.7	9.7	8.1	7.1	5.6	3.0
50	4.6	17.3	15.7	14.2	12.2	11.2	9.7	8.6	7.1	4.6
60	6.1	18.8	17.3	15.7	13.7	12.7	11.2	10.2	8.6	6.1
70	8.9	21.6	20.1	18.5	16.5	15.5	14.0	13.0	11.4	8.9

a range of peak application rates. Of course, the hydraulic conductivity can be quite variable, and users should consider a range of values for the irrigation design scaling factor when evaluating the suitability of a sprinkler package for a given soil texture class.

The NRCS has developed recommendations for surface storage based on the soil slope and the amount of crop residue covering the soil surface (table 3). The values for the effect of slope are derived from the initial work of Dillon et al. (1972). We recommend caution when using surface storage in excess of 15 mm, even for relatively flat land and high residue levels.

DESIGN AND MANAGEMENT GUIDELINES

These results can be used to develop guidelines for the design and management of center pivots to minimize runoff. The guidelines are based on selection of a sprinkler package and management so that there is no runoff, i.e., surface storage equals the amount of applied water that exceeds the infiltration rate. The fraction of the water application to be stored on the soil surface for values of α and β are presented in the upper portion of figure 5. The lower portion of figure 5 provides the ratio of the wetted radius for the sprinkler package to the radial distance from the pivot base for combinations of α and the ratio of the system capacity to the effective hydraulic conductivity. These dimensionless relationships can be used to select sprinkler packages. For example, suppose a producer:

- Applies 25 mm per application.
- Has a field with a slope of 1.5% and 10% residue cover.
- Has silt loam soil with an effective hydraulic conductivity of 7 mm h^{-1}.
- Irrigates when the root zone reaches 50% management allowed depletion.
- Has a gross system capacity of 10 mm d^{-1}.

From table 3, the surface storage will be about 10 mm, so the ratio of surface storage to application depth is 0.4, as shown for example 1 in figure 5. From table 2, the value of

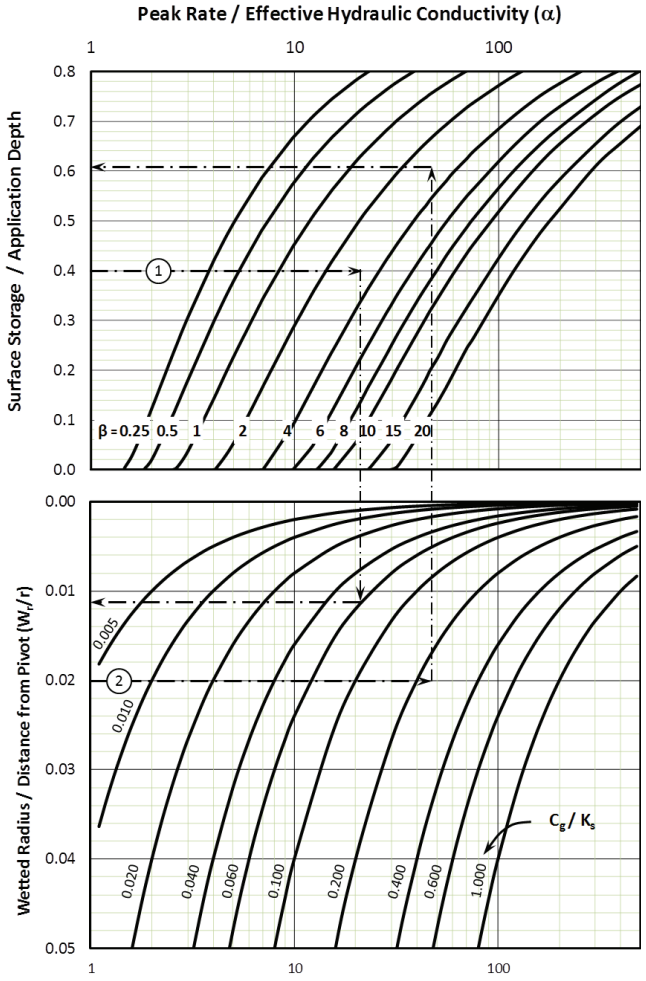

Figure 5. Solution for required wetted radius of sprinkler package relative to the radial distance from the pivot.

β is about 3.4. The ratio of system capacity to effective hydraulic conductivity is about 0.06. The ratio of the minimum wetted radius to the distance from the pivot base should be about 0.011 to avoid runoff. If concern for runoff is at the distal end of a center-pivot lateral that is 400 m long, then the sprinkler package should have at least 4.5 m of wetted radius. Sprinkler devices that provide a wetted radius larger than 4.5 m should be acceptable for this installation.

The method can also be used to determine the amount of surface storage needed for a specific sprinkler package. For example suppose:

- The wetted radius of the sprinkler package is 8 m and the system is 400 m long.
- The soil is a silty clay loam with an effective hydraulic conductivity of 1.5 mm h^{-1}.
- The β value is 3.7 for 50% management allowed depletion and an application depth of 25 mm.
- The system capacity is 8 mm d^{-1}.

As illustrated in example 2 in figure 5, the ratio of the wetted radius to the radial distance is 0.02, and the ratio of the system capacity to the effective hydraulic conductivity is 0.22. When combined with the β value of 3.7, the results show that the irrigator should plan for surface storage equal to about 60% of the application depth, or 15 mm. This will require level fields and high levels of residue.

The method can also be used to develop charts for specific soils, as illustrated for a silt loam soil in figure 6. This chart is based on the capillary drive from Rawls et al. (1982). Users could enter local soil properties if they are available. An example is included in the figure for an application depth of 25 mm, surface storage of 10 mm, and system capacity of 8 mm d^{-1}. For this example, the minimum required wetted radius would be about 5.5 m to avoid runoff at a radial distance 400 m from the pivot base.

Comparing the results in figure 6 to example 1 in figure 5 illustrates the significance of the capillary drive to sprinkler package selection. The input parameters are the same, except that example 1 uses a capillary drive of 342 mm and figure 6 is based on a capillary drive of 200 mm for the silt loam soil. For a system capacity of 10 mm d^{-1}, as used in example 1, the minimum wetted radius from figure 6 would be about 7 m.

We have developed solutions for these applications in a spreadsheet format. We also prepared graphs that allow for visual analysis of the relationships. It is relatively easy to evaluate the sensitivity of various inputs when using the graphical solutions. This is especially important for parameters that are uncertain, such as effective hydraulic conductivity, capillary drive, and surface storage. Drawing a few lines on the figures allows for a quick visual inspection of the sensitivity of various parameters on the design and management guidelines.

DROPLET EVAPORATION

Previous research has shown that the droplet size is very important to the performance of sprinkler systems. Sprinkler droplet size distributions were determined for five sprinkler devices using coefficients presented by Kincaid et al. (1996). Sprinkler devices simulated for this example were impact sprinklers, Senninger Wobbler, Nelson Rotator with a D4 pad, Nelson Spray I with a concave plate, and Nelson Spray I with a flat smooth plate. Specific design parameters are listed in table 4. Droplet distribution patterns were determined using the DPEVAP model of Thompson et al. (1993a). The Cupid-DPE model (Thompson et al., 1993b) was used to simulate crop-water balance during sprinkler irrigation for a corn canopy using weather data for McCook, Nebraska, on July 6, 1995.

Water loss distribution was simulated for each sprinkler device located approximately halfway along the lateral for a 53 ha field irrigated with a center-pivot system. The application rate pattern for each sprinkler device was based on a total application depth of 25 mm. This required a 72 h rotation time with a system flow rate of 50.7 L s^{-1}. Impact sprinklers were spaced 9.14 m apart along the lateral, while spray devices were spaced at 2.75 m. Impact sprinklers used a 16 mm diameter nozzle with an operating pressure of 411 kPa. All spray devices used an operating pressure of 138 kPa with a 5.2 mm diameter nozzle. Wind speed was referenced to an elevation of 2 m and extrapolated above the plant canopy using a log-wind profile. Sprinklers were

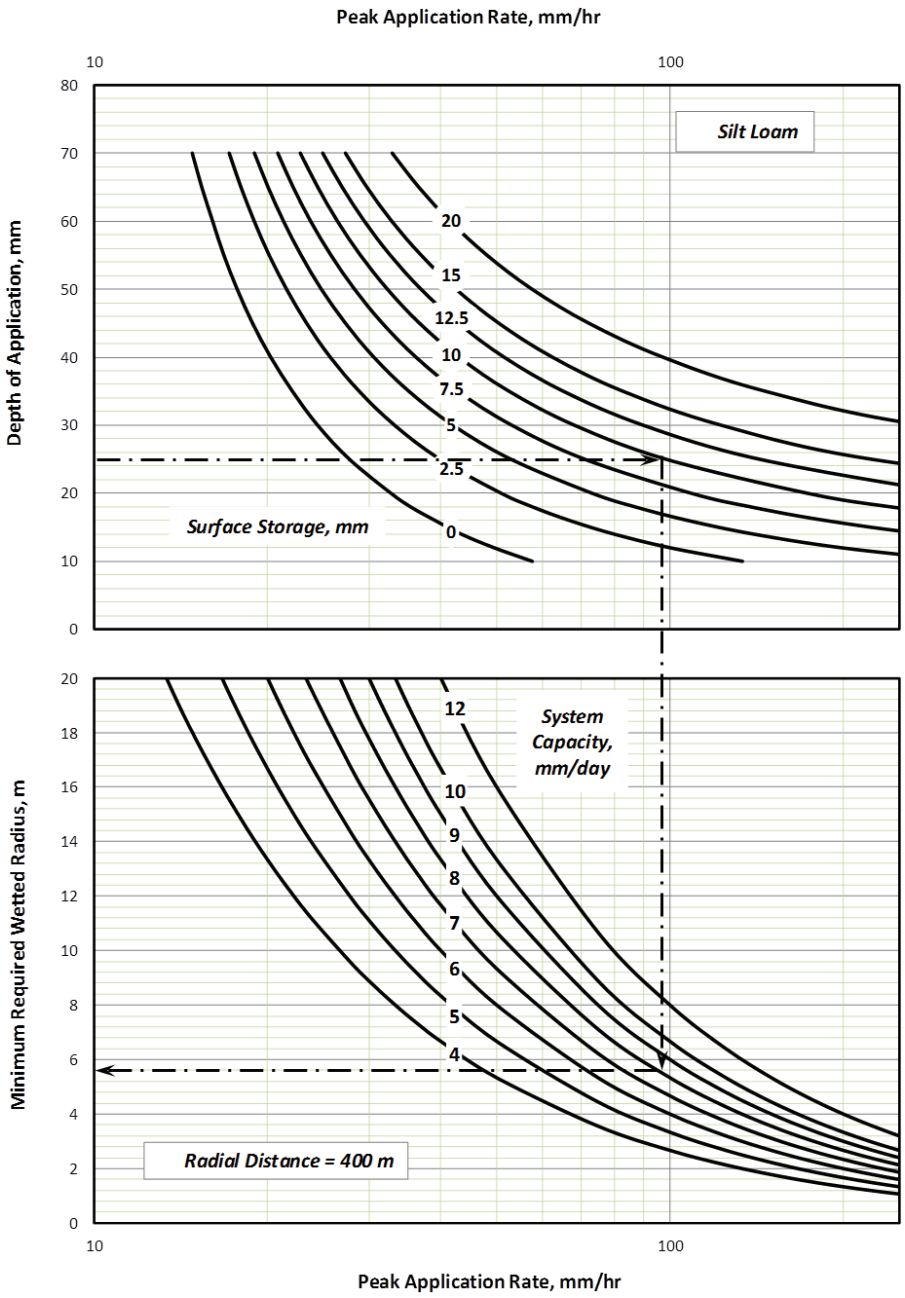

Figure 6. Solution of minimum wetted radius for a silt loam soil based on the capillary drive from Rawls et al. (1982).

assumed to be 4.3 m above the soil surface, and during the first week of July the corn canopy was assumed to be 1.4 m tall. In the second set of simulations, the spray devices were assumed to be inverted on drop tubes and positioned 2.75 m above the soil surface.

Droplet size distributions for each sprinkler device are shown in figure 7. The flat smooth spray plate had the smallest mean and maximum droplet sizes of the five devices. The average droplet size increased for the other devices in the following order: concave spray devices, Wobbler, Rotator, and impact sprinkler. Depending on sprinkler placement and trajectory angle, sprinklers with the smallest droplets would be expected to have the greatest potential for drift and direct evaporation loss (Thompson et al., 1993b).

The simulated application rates for devices placed atop the pivot lateral (4.3 m above the soil surface) are shown in figure 8. The application rates increased when spray devices were suspended on drop tubes 2.75 m above the soil surface, as shown in figure 9. The wetted radius of the impact sprinkler atop the lateral exceeded 16 m, resulting in an application time (time of wetting) of 110 min. In com-

Table 4. Sprinkler and nozzle-plate devices used in model simulations.

Sprinkler	Type	Trajectory Angle (approx. deg.)
Impact	Straight bore	25
Senninger Wobbler	Six-groove plate	30
Nelson Rotator D4	Four-groove plate	8
Nelson Spray I	Concave 30-groove plate	6
Nelson Spray I	Flat smooth plate	0

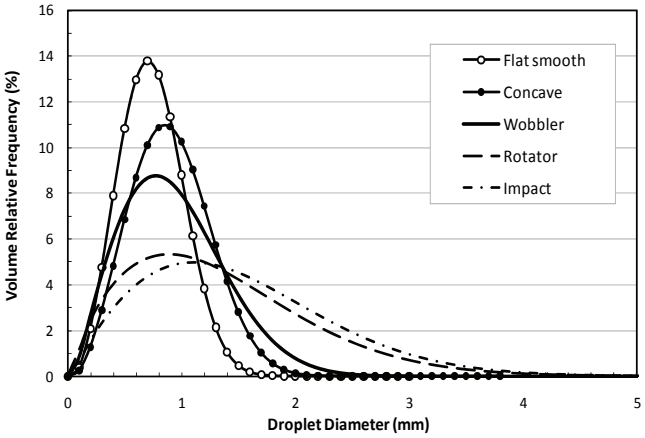

Figure 7. Droplet size volume relative frequency distribution for sprinkler devices.

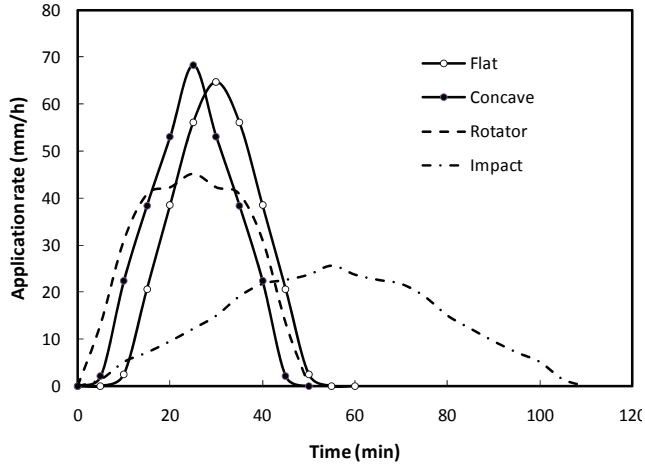

Figure 8. Simulated application rate with devices atop the pivot lateral, 4.3 m above soil surface.

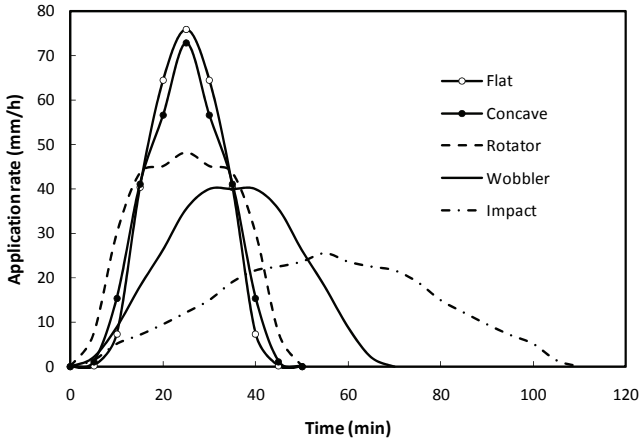

Figure 9. Simulated application rate with devices on drop tubes, 2.75 m above soil surface. The rate for the impact sprinkler mounted atop the lateral 4.3 m above the ground is included for comparison.

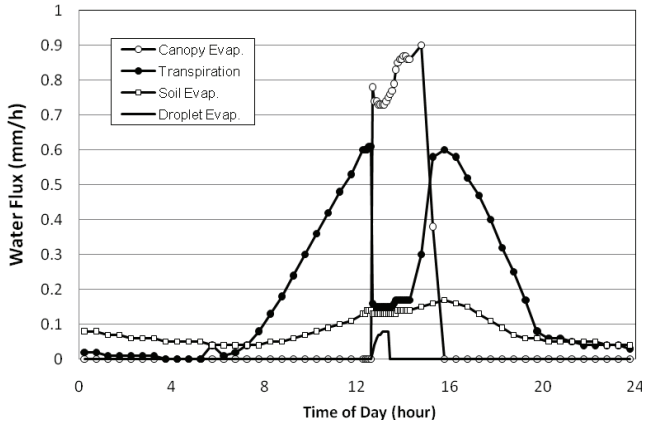

Figure 10. Water use for the Rotator sprinkler placed on top the pivot lateral.

parison, the wetted radii was smaller for all spray devices, ranging from 70 min for the Wobbler on drop tubes to about 40 min for stationary spray pad devices. Maximum application rates ranged from 68 mm h^{-1} for stationary pad spray devices to 26 mm h^{-1} for the impact sprinkler. The application rates of most spray devices increased due to smaller wetted diameters when the devices were inverted and placed on drop tubes. The smallest peak application rate for the spray devices was 50% higher than for the impact sprinkler.

The Cupid-DPEVAP model was used to simulate evaporative water loss for each sprinkler device. Five consecutive days were simulated, with irrigation on the fourth day (July 6). Results for the day of irrigation are shown in table 5, with water losses separated into canopy evaporation, transpiration, soil evaporation, and droplet evaporation. The total evaporative loss was highest at 8.54 mm d^{-1} for the impact sprinkler. The smallest loss occurred for the Rotator placed on drop tubes. However, the difference between these two extremes is less than 4% (0.28 mm) for the day. Soil evaporation is essentially the same for all sprinkler devices and placements.

The water balance components during the day are shown in figure 10 for the Rotator placed on top of the lateral. Irrigation began just after noon and lasted for 50 min. Note that the dominant water loss during irrigation was canopy evaporation, which consequently suppressed transpiration. The large initial rate of canopy evaporation occurred in part

Table 5. Water distribution for sprinklers atop the pivot lateral and on drop tubes.

Sprinkler Type	Drop Tube	Droplet Evaporation (mm)	Canopy Evaporation (mm)	Transpiration (mm)	Soil Evaporation (mm)	Total ET (mm)
Impact	No	0.04	2.42	4.14	1.93	8.54
Wobbler	Yes	0.03	1.91	4.49	1.91	8.35
Rotator	No	0.05	1.96	4.54	1.92	8.47
	Yes	0.03	1.46	4.84	1.93	8.26
Concave	No	0.06	1.64	4.70	1.91	8.30
	Yes	0.03	1.65	4.81	1.93	8.41
Flat-smooth	No	0.09	1.67	4.69	1.92	8.36
	Yes	0.03	1.57	4.85	1.93	8.39

Table 6. Surface storage (mm) needed to avoid runoff for soil and sprinkler device combinations for a 25 mm application (NR indicates that runoff is unlikely for the specific soil and device combination).

Textural	Device Installed atop Lateral				Device Suspended on Drop Tubes			
Class	Flat Spray	Concave Spray	Rotator	Impact	Flat Spray	Concave Spray	Wobbler	Rotator
Sand	NR	NR	NR	NR	NR	NR	NR	NR
Loamy sand	NR	NR	NR	NR	NR	NR	NR	NR
Sandy loam	NR	NR	NR	NR	NR	NR	NR	NR
Loam	2.0	2.3	NR	NR	3.3	2.9	NR	NR
Silt loam	3.2	3.4	0.3	NR	4.4	4.0	NR	0.7
Sandy clay loam	10.4	10.6	7.5	2.7	11.4	11.1	6.5	8.0
Clay loam	13.7	13.9	11.4	7.4	14.5	14.3	10.6	11.8
Silty clay loam	13.6	13.8	11.3	7.4	14.4	14.2	10.6	11.8
Sandy clay	17.0	17.1	15.3	12.3	17.6	17.4	14.8	15.6
Silty clay	17.7	17.8	16.2	13.4	18.2	18.0	15.6	16.4
Clay	19.3	19.4	18.1	15.9	19.7	19.6	17.7	18.3

due to the initially warmer leaf temperatures, which cool relatively quickly as water evaporates from their surface. Although droplet evaporation occurred, the relatively short fall distances and flight times (most less than 3 s) tended to keep direct droplet evaporation low, shifting instead to canopy evaporation. Mature corn leaves can hold water films of 0.1 to 0.15 mm thickness that continue to evaporate for up to 60 min after irrigation has ceased (Thompson et al., 1997). Sprinkler devices with larger wetted diameters, and therefore that wet the canopy for longer periods, result in increased canopy evaporation. Droplet evaporation increases for sprinklers with steeper body angles and placement heights due to the increased flight times.

An additional aspect that can influence water loss is sprinkler droplet drift due to wind. Although distortion of water application was not included in the application rate patterns used for these simulations, drift was simulated for the impact sprinkler. Wind speed during the day of irrigation was approximately 5 m s^{-1} and was used to evaluate the shift in water application pattern of the sprinkler wetted radius for the pivot oriented parallel and normal to the wind. When the lateral was parallel to the wind, the wetted radius increased nearly 70%, from 16 m to over 27 m. When the pivot was oriented normal to the wind, the wetted radii was shortened slightly, with the larger effect being that the overall application uniformity was skewed to the downwind side of the sprinklers. Canopy evaporation is larger than other forms of evaporative loss. Therefore, larger overall losses would be likely if the duration of leaf wetness increased because drift wetted a larger areal portion of the canopy.

The peak rate from the simulated application patterns in figures 7 and 8 can be used with the soil characteristics in tables 1 and 2 along with the results in figure 5 to evaluate the potential for runoff. The amount of surface storage required to avoid runoff for the simulated sprinkler devices and depths used in the analysis of the evaporation potential are listed in table 6. This analysis was based on a total application depth of 25 mm and soil that was initially at a MAD level of 50%.

The combination of the runoff and evaporation analysis for these examples shows that runoff is of minor significance for soils ranging from sands through silt loam. Thus, for these soils, one would opt for sprinkler packages that minimize evaporative losses. Runoff is more problematic for the remaining soils that have higher clay contents. Significant surface storage will be necessary for these soils, and runoff is more likely if residue levels are low or slopes are significant. For these soils, avoiding runoff is more likely the overriding concern, and the savings in evaporation may be of less interest.

SUMMARY AND CONCLUSION

We have developed and continue to enhance a model of the performance of center-pivot irrigation systems. A dimensionless solution to the Green-Ampt infiltration procedure is presented to estimate runoff under center pivots. The solution shows that two scaling factors are needed to describe the runoff potential for a selected soil. One scaling factor is based on system design, while the second factor depends on irrigation management (namely, the depth of water applied and the soil water depletion at the time of irrigation).

The evaporation component of the model predicts the amount of evaporation while droplets are in the air, evaporation from the wetted canopy and soil, and the amount of transpiration. Results show that transpiration rates decline while the canopy is wet, that evaporation of droplets in the air is small, and that canopy evaporation is the dominant flux during and immediately after irrigating.

We analyzed the performance of four sprinkler packages mounted on top of the pivot lateral and four packages suspended on drop tubes for a typical midsummer day. During the middle of the growing season, evaporation from the soil is minimally affected by the type of package or the height at which the sprinkler devices are positioned. Evaporative losses are generally greater for sprinkler devices that apply water for a longer time due to a larger wetted radius.

Combining runoff and evaporative loss estimates in the same model is important to illustrate the tradeoffs in sprinkler package selection. Sprinkler packages that apply water over a wider wetted radius generally produce less runoff; however, these devices also typically have higher evaporative losses. Combining the analysis of both processes lets us compare tradeoffs in a general way and for specific field conditions. Our analysis depends on the droplet size distribution and initial trajectory of droplets for sprinkler devices. This information is not readily available for many newer models of sprinkler devices. Research to develop those relationships will enhance application of our methodology in the future.

References

Bai, S. 2001. Simulation of potential runoff from center pivot irrigation systems. MS thesis. Lincoln, Neb.: University of Nebraska.

DeBoer, D. W., and S. T. Chu. 2001. Sprinkler technologies, soil infiltration, and runoff. *J. Irrig. Drain. Eng.* 127(4): 234-239.

DeBoer, D. W., A. Moshref-Javadi, and S. T. Chu. 1988. Application of the Green-Ampt infiltration equation to sprinkler irrigation management. *Appl. Agric. Res.* 3(3): 128-132.

Delirhasannia, R., A. A. Sadraddini, A. H. Nazemi, D. Farsadizadeh, and E. Playan. 2010. Dynamic model for water application using centre pivot irrigation. *Biosystems Eng.* 105(4): 476-485.

Dillon, Jr., R. C., E. A. Hiler, and G. Vittetoe. 1972. Center-pivot sprinkler design based on intake characteristics. *Trans. ASAE* 15(5): 996-1001.

FRIS. 2008. Farm and Ranch Irrigation Survey. Volume 3—Special studies—Part 1. AC-07-SS-1. Washington, D.C. USDA National Agricultural Statistics Service. Available at: www.agcensus.usda.gov/Publications/2007/Online_Highlights/Farm_and_Ranch_Irrigation_Survey/FRIS.txt.

Gilley, J. R. 1984. Suitability of reduced pressure center pivots. *J. Irrig. Drain. Eng.* 110(1): 22-34.

Hachum, A. Y., and J. F. Alfaro. 1980. Rain infiltration into layered soils: Prediction. *J. Irrig. Drain. Eng*. 106(4): 311-319.

Heermann, D. F., and K. M. Stahl. 2006. *CPED: Center Pivot Evaluation and Design (CPED): Users' Manual.* Ft. Collins, Colo.: USDA-ARS Water Management Research Unit.

Heermann, D. F., G. W. Buchleiter, and K. M. Stahl. 1999. Effect of application pattern shape on center pivot irrigation uniformity. In *Proc. Irrigation Association Tech. Conf.* , 69-76. Fall Church, Va.: Irrigation Association.

Kincaid, D. C., D. F. Heermann, and E. G. Kruse. 1969. Application rates and runoff in center-pivot sprinkler irrigation. *Trans. ASAE* 12(6): 790-794.

Kincaid, D. C., K. H. Solomon, and J. C. Oliphant. 1996. Drop size distributions for irrigation sprinklers. *Trans. ASAE* 39(3): 839-845.

Kozak, J. A., and L. R. Ahuja. 2005. Scaling of infiltration and redistribution of water across soil textural classes. *SSSA J.* 69(3): 816-827.

Luz, P. B., and D. F. Heermann. 2005. A statistical approach to estimating runoff in center pivot irrigation with crust conditions. *Agric. Water Mgmt.* 72(1): 33-46.

NRCS. 2005. National Irrigation Guide. Part 652: Nebraska Amendment. 210-VI-NEH-IG, Amend NE4. Washington, D.C.: USDA National Resources Conservation Service. Available at: http://efotg.sc.egov.usda.gov//references/public/NE/NE_Irrig_Guide_Index.pdf.

Rawls, W. J., D. L. Brakensiek, and K. E. Saxton. 1982. Estimation of soil water properties. *Trans. ASAE* 25(5): 1316-1320.

Silva, L. L. 2007. Fitting infiltration equations to centre-pivot irrigation data in a Mediterranean soil. *Agric. Water Mgmt.* 94 (1-3): 83-92.

Thompson, A. L., J. R. Gilley, and J. M. Norman. 1993a. A sprinkler water droplet evaporation and plant canopy model: I. Model development. *Trans. ASAE* 36(3): 735-741.

Thompson, A. L., J. R. Gilley, and J. M. Norman. 1993b. A sprinkler water droplet evaporation and plant canopy model: II. Model application. *Trans. ASAE* 36(3): 743-750.

Thompson, A. L., D. L. Martin, J. M. Norman, J. A. Tolk, T. A. Howell, J. R. Gilley, and A. D. Schneider. 1997. Testing of a water loss distribution model for moving sprinkler systems. *Trans. ASAE* 40(1): 81-88.

Valin, M. I., and L. S. Pereira. 2006. DEPIVOT, A simulation model for design and performance assessment of center pivot irrigation systems. In *Proc. XVI CIGR World Congress: Agricultural Engineering for a Better World*, Paper No. 0009. Dusseldorf, Germany: VDI Verlag.